Applied Catalysis B: Environmental 91 (2009) 634–639

Contents lists available at ScienceDirect

Applied Catalysis B: Environmental

journal homepage: www.elsevier.com/locate/apcatb

Exposed crystal surface-controlled rutile TiO_2 nanorods prepared by hydrothermal treatment in the presence of poly(vinyl pyrrolidone)

Eunyoung Bae, Teruhisa Ohno *

Department of Materials Science, Faculty of Engineering, Kyushu Institute of Technology, 1-1 Sensuicho, Tobata-ku, Kitakyushu 804-8550, Japan

ARTICLE INFO

Article history:
Received 27 April 2009
Received in revised form 22 June 2009
Accepted 30 June 2009
Available online 8 July 2009

Keywords:
Photocatalyst
PVP
Rutile
Exposed crystal surface
Hydrothermal treatment

ABSTRACT

Rutile TiO_2 particles with specific exposed crystal faces were prepared by hydrothermal treatment of titanium trichloride ($TiCl_3$) solution with poly(vinyl pyrrolidone) (PVP) as a shape-control reagent. Crystal phase, shape, and size of TiO_2 particles were found to be greatly dependent on the concentration of PVP in the solution. The exposed crystal surface of TiO_2 was controlled by changing the concentration of PVP in $TiCl_3$ and NaCl solutions. The prepared TiO_2 particles were characterized by TEM, SEM, XRD, and specific surface area measurements. The photocatalytic activity of the synthesized TiO_2 particles was evaluated by decomposition of acetaldehyde and toluene in gas phase. The synthesized TiO_2 particles showed higher photocatalytic activity for degradation of acetaldehyde and toluene than did commercial TiO_2 particles (MT-600B). However, the tendency of photocatalytic activities of the synthesized TiO_2 particles for degradation of acetaldehyde in gas phase was different from that for degradation of toluene. From the photodeposition of Pt and PbO_2, we propose that the (1 1 0) face provides reductive sites and that the (1 1 1) face provides oxidative sites. The results suggest that the crystal faces facilitate the separation of electrons and holes, resulting in improvement in photocatalytic activity.

1. Introduction

Among transition-metal oxide materials, nanostructured TiO_2 has been intensively investigated in the past several decades as a select platform on which an exceptionally wide range of appealing solid-state physical–chemical properties coexist with the potential for low cost and environmental remediation and energy technologies [1–3]. Rutile TiO_2 has some advantages over anatase such as higher chemical stability and higher refractive index. It is of fundamental significance to explore mild synthetic techniques by which particle shapes, nano- and micro-meter-scale morphologies, and crystallinity are well defined and controlled [3–5]. Moreover, surface chemistry of single crystalline rutile particles has been the subject of intensive studies because their chemical activity depends greatly on surface structures [6].

Photocatalytic reaction on TiO_2 is induced by excited electrons and positive holes, which migrate in the bulk and induce reduction and oxidation, respectively, by reacting with adsorbed materials on the surface. However, recombination, which is promoted by impurities or defects, may occur on the surface or in the bulk [7]. It has been reported that well-crystallized faceted particles showed enhanced photocatalytic activity compared to particles with poorly crystalline surfaces and that the photocatalytic activity increased with increase in crystallite size, the surface itself being an intrinsic defect [8]. In our previous study, we synthesized well-crystallized and well-faceted TiO_2 nanorods as a consequence of the ripening processes occurring under hydrothermal conditions [9].

Phase-controlled synthesis of TiO_2 nanostructures is particularly challenging in liquid media, in which transformation of molecular precursors is affected by a complex interplay of thermodynamic and kinetic factors [10]. Several groups have reported methods for preparing TiO_2 particles with specific exposed crystal faces using organic and inorganic reagents [4,11]. However, there have been few reports in which the relationship between surface structure and photocatalytic activity was described [12,13]. Recently, hydrophilic polymers, such as poly(vinyl alcohol) (PVA) and poly(vinyl pyrrolidone) (PVP), have been used as shape-control reagents of metal and metal oxide particles [13–15]. Polymers are widely used in the chemical synthesis of colloidal nanocrystals, and their roles are generally documented as steric stabilizers or capping agents to protect the product from agglomeration [16]. PVP has received special attention because of its high chemical stability, nontoxicity, and excellent solubility in many polar solvents [16,17]. PVP is widely used for shape-controlled nanoparticle synthesis due to its preferred adsorption on specific surfaces [15,18]. Our results

* Corresponding author. Tel.: +81 93 884 3318; fax: +81 93 884 3318.
E-mail address: tohno@che.kyutech.ac.jp (T. Ohno).

0926-3373/$ – see front matter © 2009 Elsevier B.V. All rights reserved.
doi:10.1016/j.apcatb.2009.06.034

suggest that the preferred adsorption of PVP is on (1 1 1) and (0 0 1) rutile crystal faces, resulting in exposure of the (0 0 1) face of TiO_2 nanorods.

In the present study, rutile TiO_2 nanorods with specific exposed crystal faces were prepared by hydrothermal treatment using aqueous $TiCl_3$ and NaCl as reactants and PVP as a shape-control reagent. The resulting products were fully characterized, and the effects of concentration of PVP on crystallinity, crystal size, and crystal shape were determined. The photocatalytic activities of different samples in the oxidation of acetaldehyde and toluene were determined and were found to be correlated with crystal shape of the rutile TiO_2 nanorods. We demonstrated that the crystal surface structure of TiO_2 nanorods can be controlled by adjusting the concentration of PVP. These TiO_2 nanorods are expected to show high levels of photocatalytic activity due to the different crystal faces.

2. Experimental

2.1. Chemicals

All of the chemical reagents used in this study were commercial products without further treatment. Titanium trichloride ($TiCl_3$), sodium chloride (NaCl), poly(vinyl pyrrolidone) (PVP-K30, molecular weight: 40,000), 2-propanol ($(CH_3)_2CHOH$), hexachloroplatinic acid ($H_2PtCl_6{\cdot}6H_2O$), lead nitrate ($Pb(NO_3)_2$), and nitric acid (HNO_3) were purchased from Wako (all of reagent grade), and acetaldehyde (CH_3CHO) and toluene were purchased from Aldrich. TiO_2 (MT-600B, Tayca), a rutile with an average surface area of 25–35 $m^2\,g^{-1}$, was used as a reference photocatalyst.

2.2. Sample preparation

In a typical synthesis procedure, a chemical solution was put in a sealed Teflon-lined autoclave reactor containing 50 ml aqueous solution of titanium trichloride ($TiCl_3$, 0.15 M), sodium chloride (NaCl, 5 M) and poly(vinyl pyrrolidone) (PVP, 0–0.5 mM). The solutions were then put into a 180 °C oven for 10 h. The substrate was centrifuged and rinsed with deionized water and then dried in a vacuum oven. After hydrothermal treatment, the organic compounds that remained or were adsorbed on the surface of TiO_2 particles were removed by ultraviolet (UV) irradiation with a 500-W super-high-pressure mercury lamp (Ushio, SX-UI501UO) for 24 h. The particles were dried under reduced pressure at 60 °C for 6 h. Throughout this paper, samples are referred to as SH5-0 PVP (without PVP), SH5-0.1 PVP (0.1 mM PVP), SH5-0.25 PVP (0.25 mM PVP), SH5-0.4 PVP (0.4 mM PVP) and SH5-0.5 PVP (0.5 mM PVP).

2.3. Photodeposition of Pt and PbO_2 on TiO_2 particles

Photodepositions of Pt and PbO_2 were carried out to determine reduction and oxidation sites on TiO_2 particles [19,20]. For Pt/TiO_2 preparation, an aqueous TiO_2 suspension (SH5-0.25 PVP) (2 g/l) containing 0.52 M 2-propanol and 1 mM hexachloroplatinic acid ($H_2PtCl_6{\cdot}6H_2O$) was irradiated with a 500 W Hg lamp (USHIO Co. Ltd., SX-UI501HQ) for 24 h. N_2 gas was vigorously purged through the suspension prior to UV irradiation. The light intensity was about 1 mW cm^{-2}. After irradiation, the color of the powder changed from white to gray, and the suspension was centrifuged and washed with distilled water and then collected as powder after drying for 3 h at 70 °C under reduced pressure.

Using this platinized TiO_2 powder, Pb^{2+} ions were oxidized into PbO_2. This reaction was carried out in an aqueous Pt/TiO_2 suspension (2 g/l) containing 0.1 M $Pb(NO_3)_2$ under aerated conditions. The pH of the solution for this reaction was adjusted to 1.0 by the addition of nitric acid according to the literature [19,20]. After photoreaction for 24 h using a 500 W Hg lamp, the color of the powder changed from gray to brown, indicating that PbO_2 had been deposited on the surface. The light intensity was about 0.1 W cm^{-2}. Pt and PbO_2 particles deposited on TiO_2 were observed in SEM, EDX and TEM images.

2.4. Characterization

Phase identification of TiO_2 particles was determined from X-ray diffraction (XRD) patterns measured with an X-ray diffractometer (JEOL, JDX3500) with Cu Kα radiation (λ = 1.5405 Å). The mean grain size (d) was determined from Scherrer's equation [13,21] ($d = 0.9\lambda/\beta\cos\theta$, where λ is the wavelength of the X-ray radiation, β is the full width at half-maximum of the diffraction peak, and 2θ is the diffraction angle). The morphology of the samples was observed by field emission scanning electron microscopy (FE-SEM; JEOL, JSM-6701FONO) and transmission electron microscopy (TEM; Hitachi, H-9000NAR). The specific surface area was determined with a surface area analyzer (Quantachrome, Autosorb-1) by using the Brunauer–Emmett–Teller method [22].

2.5. Photocatalytic activity measurement

The photocatalytic activity of TiO_2 nanoparticles was evaluated by measuring the changes in concentrations of acetaldehyde and toluene and evolved CO_2 as a function of irradiation time. A Tedlar bag (AS ONE Co. Ltd.) was used as the photoreactor vessel. One hundred mg of TiO_2 powder was spread on the bottom of a glass dish and the dish was placed in a reaction vessel with a volume of 125 cm^3. Then 500 ppm of acetaldehyde was prepared in the vessel by injection of saturated gas acetaldehyde or 100 ppm of toluene was prepared in the vessel by injection of saturated gas toluene. Irradiation was conducted at room temperature after equilibrium between the gas and adsorbed acetaldehyde or toluene had been reached. The light source was a 500 W Xe-lamp (USHIO Co. Ltd., SX-UI501XQ). The light beam was passed through a UV-35 filter to cut off wavelength shorter than 350 nm. Fine stainless meshes were used as neutral density filters to adjust the irradiation intensity (30 mW cm^{-2}). After starting the irradiation, the decrease in acetaldehyde concentration and evolved carbon dioxide concentration was measured using a gas chromatograph (Shimadzu Model GC-8A and GC 14A) equipped with a Flame Ionization Detector (FID). Toluene was analyzed by a gas chromatograph (Shimadzu GC-1700AF) equipped with an FID and a TC-1 capillary column (length, 30 m; i.d., 0.25 mm; film thickness, 0.25 μm).

3. Results and discussion

3.1. XRD patterns and specific surface area of rutile nanorods

Fig. 1 shows XRD patterns of TiO_2 particles prepared by hydrothermal treatment with PVP at 180 °C for 10 h. All of the diffraction peaks in the XRD patterns agree with those of TiO_2 in rutile form and no other phases were detected. The intensity of diffraction peaks of rutile TiO_2 becomes stronger with increase in PVP concentration, indicating improvement in crystallinity of the rutile rod as shown in Fig. 1. Scherrer's equation was applied to the rutile (1 1 0) peaks and provided a mean grain size of around 50–55 nm for prepared TiO_2 (as shown in Table 1). These results indicated that the crystal sizes of the resulting rutile nanorods increased with increase in the concentration of PVP. The specific surface areas of samples are shown in Table 1. BET surface area increased with increase in the concentration of PVP.

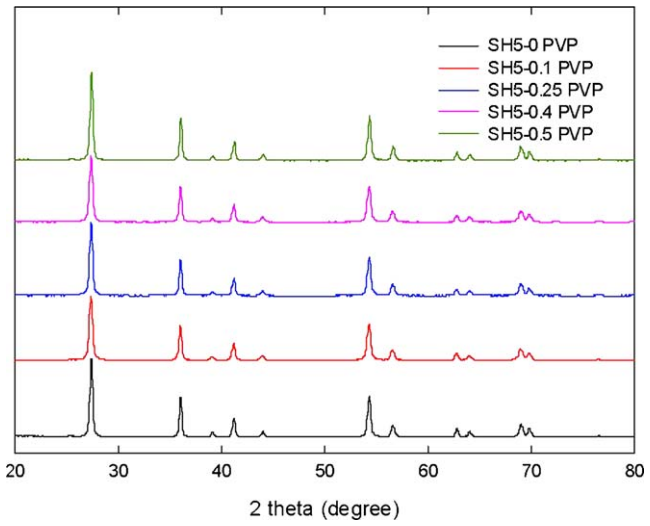

Fig. 1. XRD patterns of samples obtained from $TiCl_3$ solutions with various concentrations of PVP after hydrothermal treatment for 10 h at 180 °C.

Table 1
Physical properties of rutile TiO_2 nanorod samples and reference TiO_2.

Sample	Synthesis conditions (M)			Mean crystallite size (nm)	BET surface area (m^2/g)
	$TiCl_3$	NaCl	PVP (mM)		
MT-600B				50	25–35
SH5-0 PVP	0.15	5	0	58.66[a]	21.84
SH5-0.1 PVP	0.15	5	0.1	47.43[a]	26.27
SH5-0.25 PVP	0.15	5	0.25	51.68[a]	27.89
SH5-0.5 PVP	0.15	5	0.5	56.02[a]	30.63

[a] Calculated as weighted mean value of the crystallite size (XRD) of TiO_2.

3.2. TEM and SEM observations of rutile nanorods

To determine the role of PVP in the reaction, we conducted a series of syntheses by varying the concentration of PVP. TEM and SEM images showed that addition of the PVP polymer resulted in perfect control of the shape of TiO_2 nanorods. Fig. 2 shows TEM images of rutile TiO_2 nanorods obtained after hydrothermal treatment with different PVP concentrations. TEM images without PVP (Fig. 2a) showed a rod-like shape with a triangular end rutile structure and single crystalline quality of the TiO_2 nanorod. TEM images with PVP (Fig. 2b–d) showed that the shape of the rod end changed from a triangular tip to a larger square tip when the concentration of PVP was increased (from 0.1 to 0.5 mM). We calculated edge sizes of the (0 0 1) direction from TEM images: SH5-0 PVP (0 nm) < SH5-0.1 PVP (15 nm) < SH5-0.25 PVP (37 nm) < SH5-0.5 PVP (69 nm). As previously reported [9], SAED patterns of the exposed surface of the end of the rod and side surface of the rod were assigned to (1 1 1) and (1 1 0), respectively (data not shown). The area of exposed (1 1 1) crystal faces gradually decreased with increase in PVP concentration. At the same time, a new crystal face assigned to the (0 0 1) face gradually became exposed as shown in Fig. 2. Consequently, surface morphology of the rutile TiO_2 rod was controlled by changing the concentration of PVP. These results indicated that chemical structure of the added PVP greatly affects the shape of the rod end of rutile TiO_2 crystals. Fig. 3 shows SEM images of samples taken from nanorods obtained with different PVP concentrations. SEM images without PVP (Fig. 3a) revealed that the structures were composed of nanorods with triangular-like tips. When the concentration of PVP was increased from 0.1 to 0.5 mM, the shape of the end of the rod changed from a triangular-like tip (composed of four triangular-shaped faces with one vertex) to a trapezoid-like tip (composed of four trapezoidal-shaped faces and one square top) (Fig. 3). The shape of the formed TiO_2 nanorods changed with change in the concentration of PVP via hydrothermal treatment. In the case of commercially available PVP, the ends of the rods are terminated with a hydroxyl (–OH) group because of the involvement of water as a polymerization medium and the presence of hydrogen peroxide [17]. The formed side surfaces, (1 1 1) facets, must be stabilized through chemical interactions with oxygen (and/or nitrogen) atoms of the pyrrolidone units of PVP. In addition, since twinning is only favorable when the surface energy of the (1 1 1) facets is greater than that of the (1 1 0) facets [6], the presence of PVP can serve to reduce the driving force for twin formation through its selective interaction with the (1 1 1) planes [18]. Thus, our results suggest that the shape of the TiO_2 nanorod is controllable by additive PVP of the solution.

3.3. Photocatalytic activity for acetaldehyde and toluene decomposition

Photocatalytic activity for acetaldehyde decomposition strongly depended on the surface structure of prepared TiO_2 nanorods. Fig. 4 shows photocatalytic evolution of CO_2 as a result of complete degradation of acetaldehyde on the prepared rutile TiO_2 nanorods prepared with PVP at light intensity of 30 mW cm^{-2}. Photocatalytic activity levels of synthesized rutile TiO_2 are much higher than those of MT-600B (reference TiO_2) and rutile TiO_2 prepared without PVP. Photocatalytic activity of the TiO_2 particles showed dependence on the concentration of PVP, though S_{BET} showed dependence on the amount of PVP. However, photocatalytic activity level of rutile TiO_2 showed a tendency to be saturated at PVP concentrations above 0.25 mM. A plausible explanation is degradation of acetaldehyde, which is easily decomposed under UV irradiation. Under this condition, injection of photoexcited electrons in the conduction band to oxygen adsorbed on the surface of TiO_2 particles should be a rate-determining step. Therefore, the photocatalytic activity of rutile TiO_2 nanorods for degradation of acetaldehyde reached an appropriate level because the amount of oxygen adsorbed on the surface of rutile TiO_2 with small relative surface area might be smaller than that of electrons generated photocatalytically in rutile TiO_2. However, toluene is a compound that it difficult to be oxidized because accumulated intermediates obtained from ring-opening reaction of toluene reduce the rate of toluene photo-oxidation [23]. We therefore showed the photocatalytic activity of toluene in gas phase compared to that of acetaldehyde. Fig. 5 shows the time course of CO_2 evolution in degradation of toluene over TiO_2 nanorods prepared with various concentrations of PVP. Photocatalytic activity levels of TiO_2 nanorods are higher than those of MT-600B as a reference TiO_2.

Photocatalytic activity levels of TiO_2 nanorods prepared with PVP are higher than those of TiO_2 nanorods prepared without PVP. Photocatalytic activity of the TiO_2 particles showed dependence on the concentration of PVP (SH5-0.25 PVP > SH5-0.4 PVP > SH5-0.5 PVP > SH5-0.1 PVP > SH5-0 PVP (without PVP) > MT-600B), though S_{BET} showed no dependence on the concentration of PVP (see Table 1). TiO_2 prepared with 0.25 mM of PVP showed the highest photocatalytic activity among the prepared TiO_2 samples despite similar surface structures. Moreover, TiO_2 particles prepared with 0.25 mM of PVP showed completely degradation of toluene, which is hardly oxidized by a TiO_2 catalyst. Unlike the case of degradation of acetaldehyde, photodegradation of toluene might be the rate-determining step. Therefore, we did not observe a tendency for saturation of photocatalytic activity for degradation of toluene in

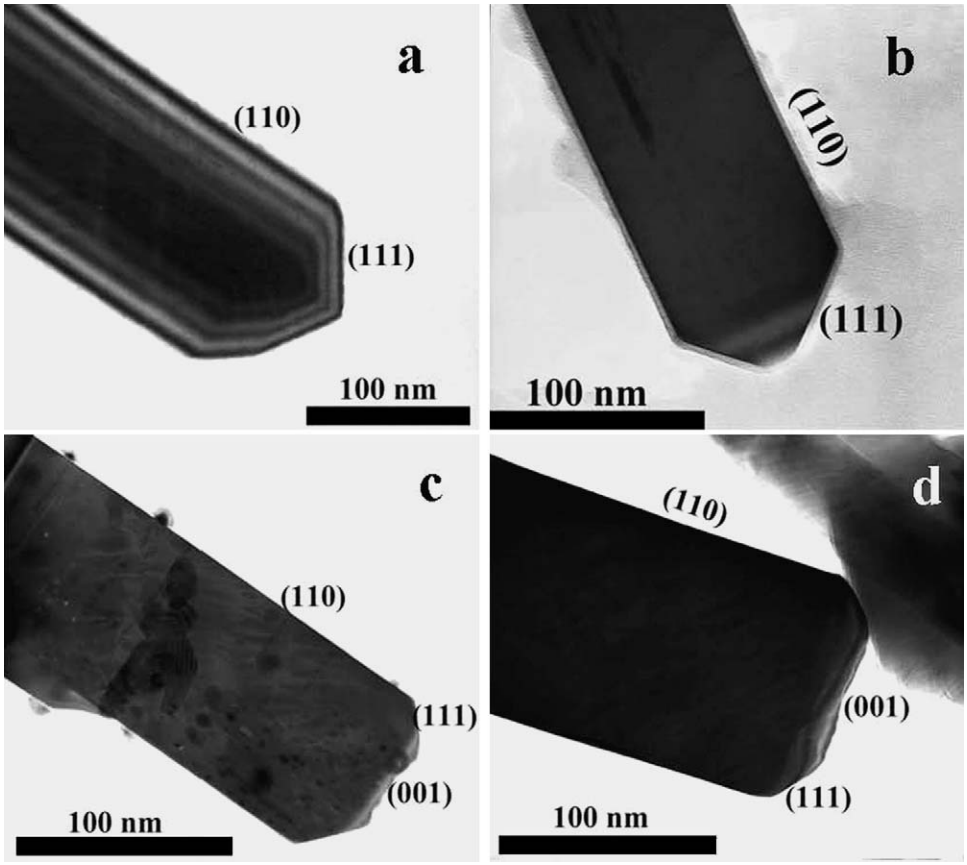

Fig. 2. TEM images of (a) SH5-0 PVP, (b) SH5-0.1 PVP, (c) SH5-0.25 PVP and (d) SH5-0.5 PVP.

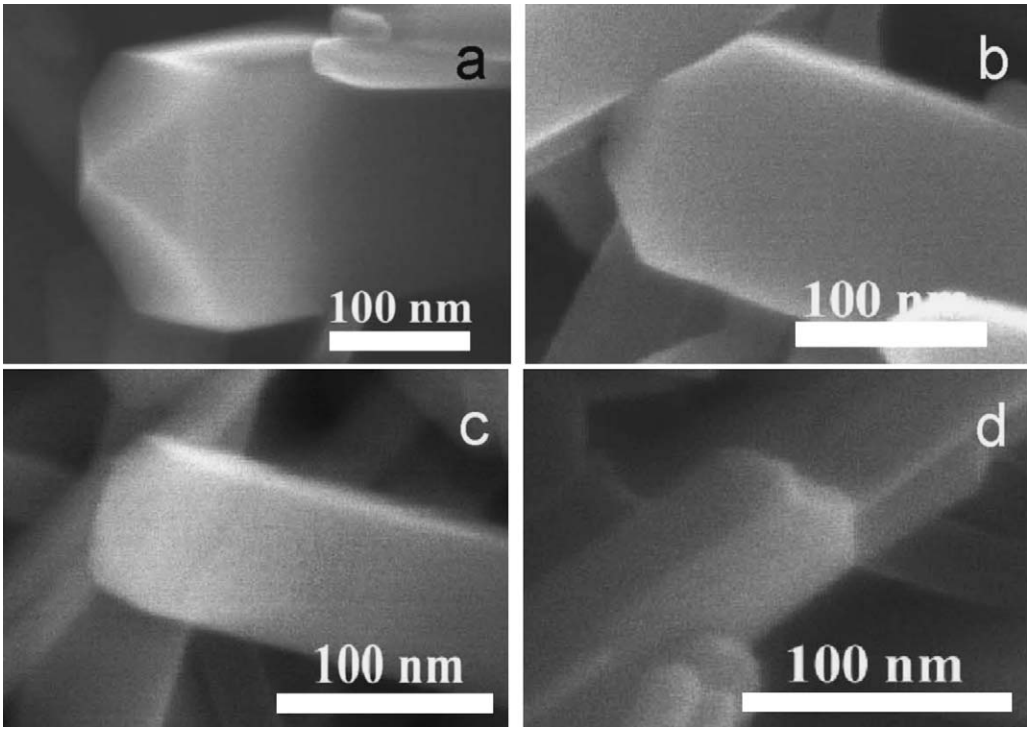

Fig. 3. SEM images of (a) SH5-0 PVP, (b) SH5-0.1 PVP, (c) SH5-0.25 PVP and (d) SH5-0.5 PVP.

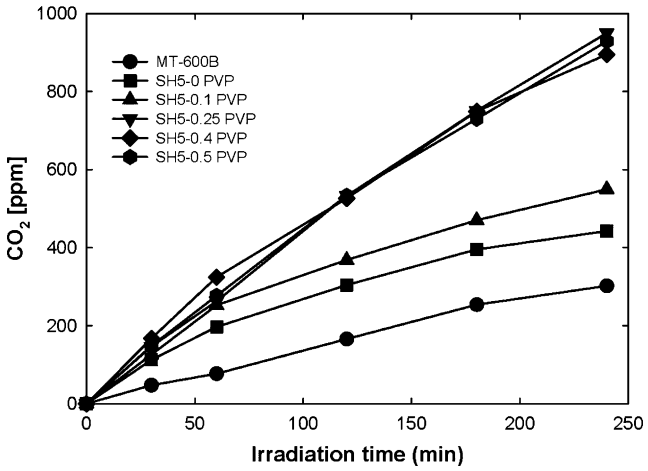

Fig. 4. Time profiles of decomposition of acetaldehyde on TiO_2 at different concentrations of PVP at light intensity of 30 mW cm^{-2}. The experimental conditions were: $[acetaldehyde]_i$ = 500 ppm, $[TiO_2]$ = 10.4 mg/cm^2, UV light ($\lambda > 350$ nm) irradiated.

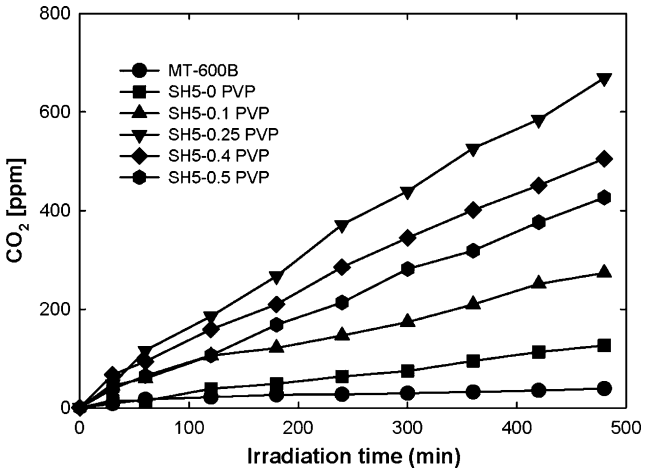

Fig. 5. Time profiles of decomposition of toluene on TiO_2 at different concentrations of PVP at light intensity 30 mW cm^{-2}. The experimental conditions were: $[toluene]_i$ = 100 ppm, $[TiO_2]$ = 10.4 mg/cm^2, UV light ($\lambda > 350$ nm) irradiated.

gas phase. That is, the activity of rutile TiO_2 for degradation of toluene changed drastically depending on the kind of rutile TiO_2 nanorods under UV irradiation. The photocatalytic activity of rutile TiO_2 nanorods was maximum when the amount of PVP was 0.25 mM. Under this condition, the new exposed crystal face, (0 0 1), was thought to play an important role in improvement of photocatalytic activity of rutile TiO_2 nanorods. We previously reported that the (1 1 1) crystal face acts as an oxidation site [9]. However, the new exposed crystal face, (0 0 1), showed stronger oxidation power than that of the (1 1 1) crystal face as can be seen in Fig. 5.

TiO_2 prepared with high concentrations of PVP (0.4 and 0.5 mM) showed lower photocatalytic activity than that of TiO_2 prepared with 0.25 mM PVP despite having similar surface structures and larger surface areas. A possible reason for this is that residual PVP adsorbed on TiO_2, which was presumably not completely removed by UV irradiation in the preparation procedure, might prevent photoabsorption and adsorption of

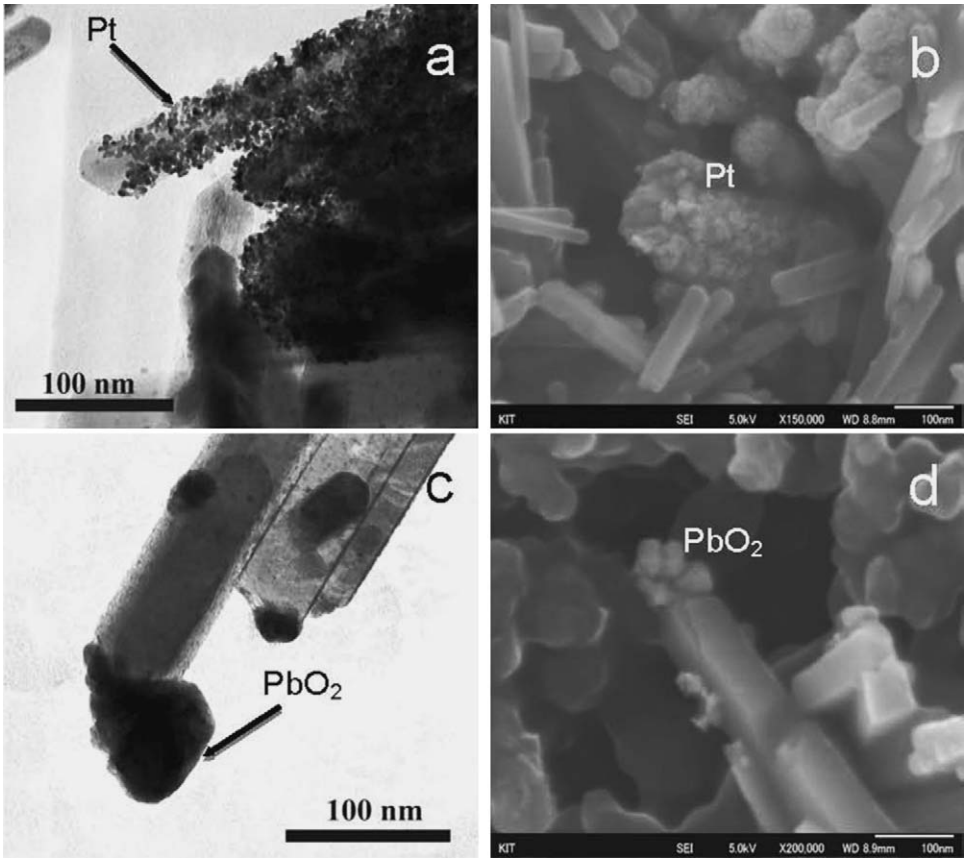

Fig. 6. TEM image (a) and SEM image (b) of a rutile TiO_2 nanorod (SH5-0.25 PVP) on which Pt particles were deposited. TEM image (c) and SEM image (d) of a rutile TiO_2 nanorod (SH5-0.25 PVP) on which Pt and PbO_2 particles were deposited.

reactants, resulting in a decrease in the efficiency of photocatalytic reaction. However, our results suggested that the photocatalytic activity of the samples for acetaldehyde and toluene degradation was affected by the new exposed crystal surface, (0 0 1), of rutile TiO_2.

The large specific surface areas and small crystal sizes as well as high crystallinity of TiO_2 might usually play important roles in the enhancement of photocatalytic activities. However, separation of reaction sites on the photocatalyst particle by the exposed crystal surface of the rutile nanorod is a more important factor for improvement of photocatalytic activity because a rutile nanorod having a small surface area (20–30 $m^2\ g^{-1}$) showed a higher level of photocatalytic activity than that of ST-01 having a large surface area (300 $m^2\ g^{-1}$) [9]. These results indicate that the charge separation between photo-excited electrons and holes should be improved by optimization of the exposed crystal surfaces for reactions resulting in increase of photocatalytic activity.

3.4. Photocatalytic deposition of Pt and PbO_2 on TiO_2 nanorods

To determine the site at which reduction or oxidation predominantly proceeds, photodeposition of Pt and PbO_2 was carried out. Fig. 6 shows TEM and SEM images of Pt- and PbO_2-deposited TiO_2 nanorods that were prepared with 0.25 mM of PVP. The deposited metals were analyzed by EDX (figure not shown). Fig. 6d shows SEM images of rutile TiO_2 particles showing PbO_2 deposits, which were loaded on the particles by UV irradiation of the Pt-deposited TiO_2 powder. Pt particles were deposited on the (1 1 0) face as shown in Fig. 6a and b. Fig. 6c and d shows that the PbO_2 particles were deposited on the (1 1 1) faces. The results shown in Fig. 6 indicate that the oxidation site and reduction site on the rutile particles are on the newly exposed (0 0 1) face and on the (1 1 0) face, respectively. These results agree with results of a previous study [9]. Therefore, the results suggest that effective separation of oxidation and reduction sites of rutile TiO_2 nanorods is an important factor for high efficiency of decomposition of acetaldehyde and toluene.

4. Conclusion

Addition of hydrophilic polymer PVP enabled control of exposed crystal faces of rutile TiO_2 nanorods in crystallization during hydrothermal treatment. Hydrothermal treatment with PVP resulted in rutile TiO_2 nanorods being well-crystallized and well-dispersed without formation of large aggregates. The morphology of rutile crystals can be controlled by changing the concentration of PVP. We showed that PVP is a polymer capping reagent capable of effectively covering (1 1 1) facets rather than (1 1 0) facets, resulting in exposure of (0 0 1) facets. Well-crystallized rutile TiO_2 synthesized with PVP possessed higher levels of CO_2 evolution activity than those of MT-600B and TiO_2 prepared without PVP under UV light irradiation. It was found that the photocatalytic activity depends on not surface area but surface structure of the TiO_2 nanorods, suggesting that electron–hole pair recombination plays an important role during the photodegradation of acetaldehyde and toluene, at least under the present experimental conditions. Recombination is apparently slower in well-faceted and large rutile nanorods, thus increasing the activity.

Acknowledgements

This work was partly supported by a grant of Knowledge of Cluster Initiative implemented by the Ministry of Education, Culture, Sports, Science and Technology (MEXT) and the New Energy and Industrial Technology Development Organization (NEDO).

References

[1] M.R. Hoffmann, S.T. Martin, W. Choi, D.W. Bahnemann, Chem. Rev. 95 (1995) 69–96.
[2] W. Choi, Catal. Surv. Asia 10 (2006) 16–28.
[3] X. Chen, S.S. Mao, Chem. Rev. 107 (2007) 2891–2959.
[4] E. Hosono, S. Fujihara, K. Kakiuchi, H. Imai, J. Am. Chem. Soc. 126 (2004) 7790–7791.
[5] N.R. Neale, A.J. Frank, J. Mater. Chem. 17 (2007) 3216–3221.
[6] X. Huang, C. Pan, J. Cryst. Growth 306 (2007) 117–122.
[7] C.A. Emilio, M.I. Litter, M. Kunst, M. Bouchard, C. Colbeau-Justin, Langmuir 22 (2006) 3606–3613.
[8] A. Testino, I.R. Bellobono, V. Buscaglia, C. Canevali, M. D'Arienzo, S. Polizzi, R. Scotti, F. Morazzoni, J. Am. Chem. Soc. 129 (2007) 3564–3575.
[9] E. Bae, N. Murakami, T. Ohno, J. Mol. Catal. A 300 (2009) 72–79.
[10] R. Buonsanti, V. Grillo, E. Carlino, C. Giannini, T. Kipp, R. Cingolani, P.D. Cozzoli, J. Am. Ceram. Soc. 130 (2008) 11223–11233.
[11] K. Kakiuchi, E. Hosono, H. Imai, T. Kimura, S. Fujihara, J. Cryst. Growth 293 (2006) 541–545.
[12] T. Taguchi, Y. Saito, K. Sarukawa, T. Ohno, M. Matsumura, New J. Chem. 27 (2003) 1304–1306.
[13] N. Murakami, Y. Kurihara, T. Tsubota, T. Ohno, J. Phys. Chem. C 113 (2009) 3062–3069.
[14] K. Yoshinaga, M. Yamauchi, D. Maruyama, E. Mouri, T. Koyanagi, Chem. Lett. 34 (2005) 1094–1095.
[15] D. Wang, J. Liu, Q. Huo, Z. Nie, W. Lu, R.E. Williford, Y.-B. Jiang, J. Am. Chem. Soc. 128 (2006) 13670–13671.
[16] B. Lim, P.H.C. Camargo, Y. Xia, Langmuir 24 (2008) 10437–10442.
[17] I. Washio, Y. Xiong, Y. Yin, Y. Xia, Adv. Mater. 18 (2006) 1745–1749.
[18] B. Wiley, Y. Sun, B. Mayers, Y. Xia, Chem. Eur. J. 11 (2005) 454–463.
[19] Y. Matsumoto, M. Noguchi, T. Matsunaga, J. Phys. Chem. B 103 (1999) 7190–7194.
[20] T. Ohno, K. Sarukawa, M. Matsumura, New J. Chem. 26 (2002) 1167–1170.
[21] T. Lindgren, J.M. Mwabora, E. Avendaño, J. Jonsson, A. Hoel, C.-G. Granqvist, S.-E. Lindquist, J. Phys. Chem. B 107 (2003) 5709–5716.
[22] C. Ribeiro, C. Vila, D.B. Stroppa, V.R. Mastelaro, J. Bettini, E. Longo, E.R. Leite, J. Phys. Chem. C 111 (2007) 5871–5875.
[23] R. Inaba, T. Fukahori, M. Hamamoto, T. Ohno, J. Mol. Catal. A: Chem. 260 (2006) 247–254.